

Supporting Information

A MnO₂ nanosheet-assisted GSH detection platform using an iridium(III) complex as a switch-on luminescent probe

Zhen-Zhen Dong,^{‡a} Lihua Lu,^{‡a,b} Chung-Nga Ko,^{‡a} Chao Yang,^{‡c}
Shengnan Li,^c Ming-Yuen Lee,^c Chung-Hang Leung^{*c} and Dik-Lung
Ma^{*a}

^aDepartment of Chemistry, Hong Kong Baptist University, Kowloon Tong, Hong Kong (China)

^bCollege of Chemistry and Pharmaceutical Sciences, Qingdao Agricultural University, Qingdao 266109, China.

^cState Key Laboratory of Quality Research in Chinese Medicine, Institute of Chinese Medical Sciences, University of Macau, Macao (China)

Corresponding author:

Dik-Lung Ma, E-mail: edmondma@hkbu.edu.hk, Tel: +852-3411-7075

Chung-Hang Leung, E-mail: duncanleung@umac.mo, Tel: +853-8822-4688;

Materials

Potassium permanganate (KMnO₄) was purchased from Peking chemical works (Beijing, China). 3-Morpholinopropanesulfonic acid (MOPS) and L-glutathione (GSH) were purchased from Sigma Aldrich (St. Louis, MO). All reagents were used as

received without further purification. All aqueous solutions were prepared with Milli-Q water ($18.2 \text{ M}\Omega \text{ cm}^{-1}$). Bovine serum albumin and human serum albumin were obtained from Sino Biological Inc. (Beijing, China). Other reagents, unless specified, were also purchased from Sigma Aldrich (St. Louis, MO).

General experimental

Mass spectrometry was performed at the Mass Spectroscopy Unit at the Department of Chemistry, Hong Kong Baptist University, Hong Kong (China). Deuterated solvents for NMR purposes were obtained from Armar and used as received. ^1H and ^{13}C NMR were recorded on a Bruker Avance 400 spectrometer operating at 400 MHz (^1H) and 100 MHz (^{13}C). ^1H and ^{13}C chemical shifts were referenced internally to solvent shift (acetone- d_6 : ^1H , 2.05, ^{13}C , 29.8). Chemical shifts are quoted in ppm, the downfield direction being defined as positive. Uncertainties in chemical shifts are typically ± 0.01 ppm for ^1H and ± 0.05 for ^{13}C . Coupling constants are typically ± 0.1 Hz for ^1H - ^1H and ± 0.5 Hz for ^1H - ^{13}C couplings. The following abbreviations are used for convenience in reporting the multiplicity of NMR resonances: s, singlet; d, doublet; t, triplet; q, quartet; m, multiplet; br, broad. All NMR data was acquired and processed using standard Bruker software (Topspin).

Cell imaging

HeLa cells were seeded into a glass-bottomed dish (35 mm dish with 20 mm) and cultured for 12 h. Before imaging, the cells were pre-treated with fresh medium or ALA (250 μM) or NEM (10 μM) for 1 h, followed by washing with phosphate-buffered saline and replacing with fresh medium or complex **1** (10 μM) + nanosheet (80 μM) for 2 h. After washing with phosphate-buffered saline for three times, cell imaging experiment was performed by a Leica TCS SP8 confocal laser scanning microscope system.

XTT assay

HeLa cells were seeded in 96-well plates with a density of 8,000 cells per well and incubated for 12 h. Complex **1** or nanosheet or complex **1** + nanosheet were added to the cells with final concentrations ranging from 0.001 μM to 10 μM for 2 or 6 h. 50 μL of the prepared XTT mixture were added into each well and incubated for another

4 h. Before starting the test, the plate was shaken for one min at room temperature in the dark. The cytotoxicity was monitored as the percentage of absorbance in a SpectraMax M5 microplate reader at a wavelength of 450 nm.

Survival and toxicity assay on zebrafish

72 hpf (hour post fertilization) wild type zebrafish embryos were distributed in a 24 well plate, with 12 embryos were distributed per well. The embryos were incubated with 1 mL of embryo medium containing various concentrations of complex **1** at 28 °C for 6 h, in which embryos in DMSO (0.1%) were served as a vehicle control. The survival and morphologic changes of the embryos were monitored at 2 hpt (hour post treatment) and 6 hpt. Embryos with heartbeat would be counted as alive, and their survival rates would be calculated accordingly. Images were captured at 40× magnifications using Olympus Spinning Disk Confocal Microscope System (IX81 Motorized Inverted Microscope [w/ZDC], IX2 universal control box, X-cite series 120, DP71 CCD Camera).

Imaging of zebrafish

Zebrafish were kept at 28 °C and maintained at optimal breeding conditions. For mating, male and female zebrafish were maintained in the same tank at 28 °C on a 12 h light/12 h dark cycle and then the spawning of eggs were triggered by giving light stimulation in the morning. Almost all the eggs were fertilized immediately. The 3-day old zebrafish were maintained in E3 embryo media (15 mM NaCl, 0.5 mM KCl, 1mM MgSO₄, 1 mM CaCl₂, 0.15 mM, KH₂PO₄, 0.05 mM Na₂HPO₄, 0.7 mM NaHCO₃, 10-5% methylene blue; pH 7.5). The zebrafish were pretreated with ALA or NEM for 1 h in E3 media at 28 °C. After washing with E3 media to remove the remaining ALA or NEM, the zebrafish were further incubated with **1** (10 μM) and MnO₂ nanosheet (80 μM) in E3 media for 2 h at 28 °C. After washing with E3 media, the zebrafish were imaged by fluorescence microscopy at TRITC channel.

Photophysical measurement

Emission spectra and lifetime measurements for complex **1** were performed on a PTI TimeMaster C720 Spectrometer (Nitrogen laser: pulse output 335 nm) fitted with a 395 nm filter. Error limits were estimated: λ (± 1 nm); τ ($\pm 10\%$); ϕ ($\pm 10\%$). All

solvents used for the lifetime measurements were degassed using three cycles of freeze-vac-thaw.

Luminescence quantum yield was determined using the method of Demas and Crosby¹ [Ru(bpy)₃][PF₆]₂ in degassed acetonitrile as a standard reference solution ($\Phi_r = 0.062$) and was calculated according to the reported equation:

$$\Phi_s = \Phi_r(B_r/B_s)(n_s/n_r)^2(D_s/D_r)$$

where the subscripts s and r refer to sample and reference standard solution respectively, n is the refractive index of the solvents, D is the integrated intensity, and Φ is the luminescence quantum yield. The quantity B was calculated by $B = 1 - 10^{-AL}$, where A is the absorbance at the excitation wavelength and L is the optical path length.

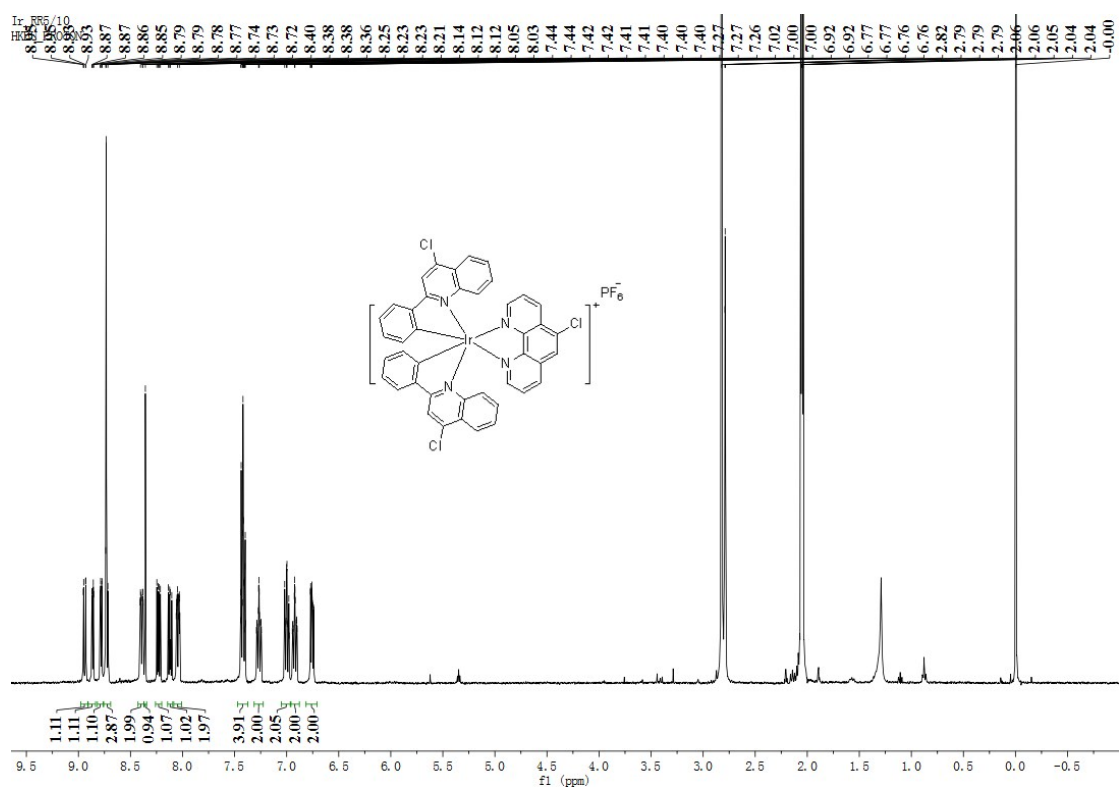
To calculate the concentration of MnO₂ nanosheets in water, the absorption spectra of the as-prepared MnO₂ nanosheets were measured and the concentration was calculated according to Lambert-Beer's Law with the molar extinction coefficient of $9.6 \times 10^3 \text{ M}^{-1} \text{ cm}^{-1}$ at 380 nm.²

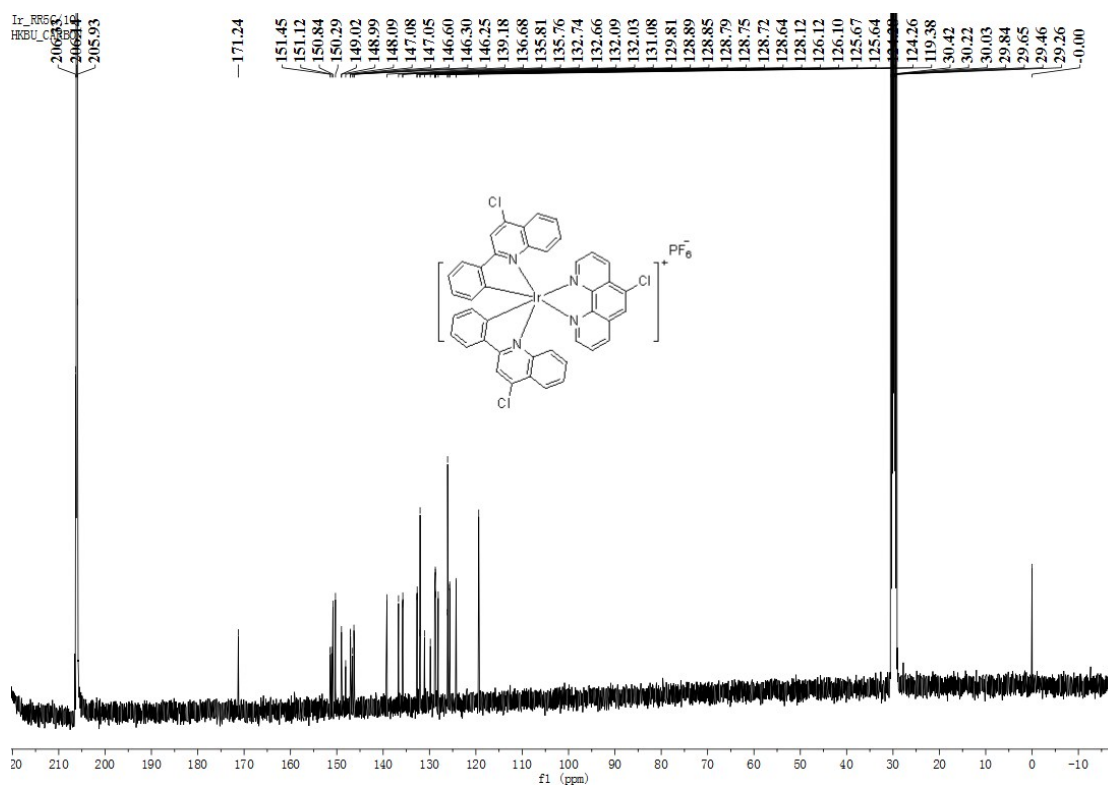
Synthesis

Complex **1** was prepared according to the (modified) literature methods.³ The precursor iridium(III) complex dimer [Ir₂(Cl-phq)₄Cl₂] (Cl-phq = 4-chloro-2-phenylquinoline) was prepared as previously reported. Then, a suspension of [Ir₂(Cl-phq)₄Cl₂] (0.1 mmol) and the corresponding N^N ligand (Cl-phen = 5-chloro-1,10-phenanthroline) (0.22 mmol) in a mixture of DCM:MeOH (1:1, 20 mL) was refluxed overnight under a nitrogen atmosphere. The work-up procedure was the same as previously reported. Complex **1** was characterized by ¹H-NMR, ¹³C-NMR, high resolution mass spectrometry (HRMS) and elemental analysis.

Complex **1** (Yield: 61%) ¹H NMR (400 MHz, Acetone-*d*₆) δ 8.94 (dd, $J = 8.5, 1.3$ Hz, 1H), 8.86 (dd, $J = 5.1, 1.4$ Hz, 1H), 8.78 (dd, $J = 5.2, 1.4$ Hz, 1H), 8.74 – 8.71 (m, 3H), 8.39 (d, $J = 7.9$ Hz, 2H), 8.36 (s, 1H), 8.25 – 8.21 (m, 1H), 8.14 – 8.10 (m, 1H), 8.08

– 8.01 (m, 2H), 7.47 – 7.37 (m, 4H), 7.27 (m, 2H), 7.00 (t, $J = 8.7$ Hz, 2H), 6.92 (t, $J = 7.3$ Hz, 2H), 6.77 – 6.74 (m, 2H). ^{13}C NMR (100 MHz, Acetone- d_6) δ 171.24, 151.45, 151.12, 150.84, 150.29, 149.02, 148.99, 148.09, 147.08, 147.05, 146.60, 146.30, 146.25, 139.18, 136.68, 135.81, 135.76, 132.74, 132.66, 132.09, 132.03, 131.08, 129.81, 128.89, 128.85, 128.79, 128.75, 128.72, 128.64, 128.12, 126.12, 126.10, 125.67, 125.64, 124.28, 124.26, 119.38. MALDI-TOF-HRMS: Calcd. for $\text{C}_{42}\text{H}_{25}\text{Cl}_3\text{IrN}_4$ $[\text{M}-\text{PF}_6]^+$: 883.0774 Found: 883.0777. Anal.: ($\text{C}_{42}\text{H}_{25}\text{Cl}_3\text{F}_6\text{IrN}_4\text{P} + 0.5\text{H}_2\text{O}$) C, H, N: Calcd. 48.59, 2.52, 5.40; found 48.47, 2.62, 5.52.





HONG KONG BAPTIST UNIVERSITY, DEPARTMENT OF CHEMISTRY (MALDI-TOF)

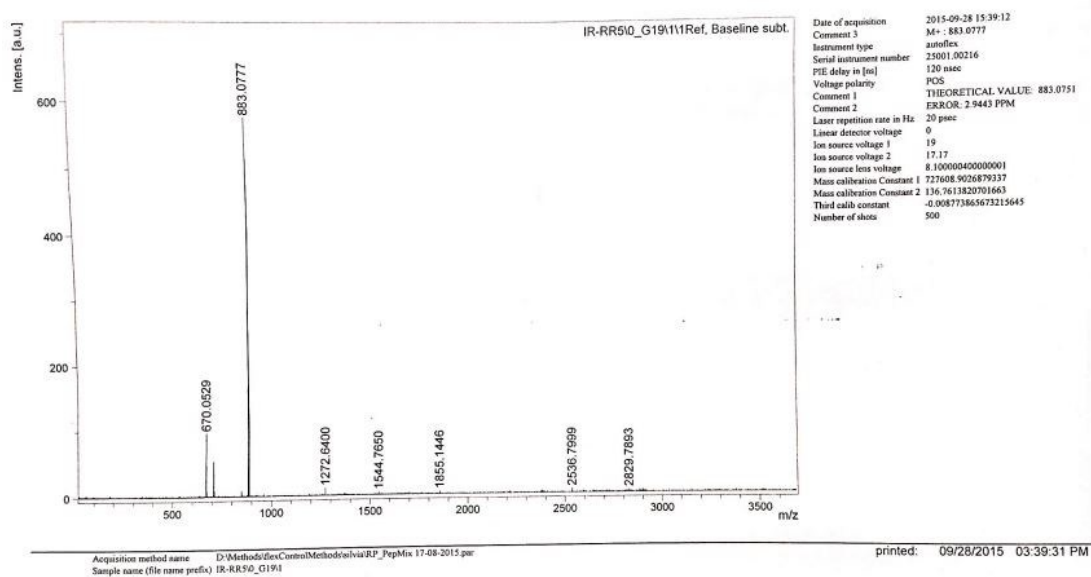


Table S1 Photophysical properties of iridium(III) complex **1** in acetonitrile (298K)

Complex	Quantum yield	λ_{ex} / nm	λ_{em} / nm	Life time / μs	UV/Vis absorption λ_{abs} / nm (ϵ / $\text{dm}^3\text{mol}^{-1}\text{cm}^{-1}$)
1	0.5747	335	583	4.718	279 (5.02×10^3), 348 (2.23×10^4), 446 (4.42×10^4)

Table S2 Comparison of the luminescent or colorimetric GSH detection assays reported in recent years.

Method	Linear range (μM)	Detection limit	Reaction time (min)	Reference
Fluorometry	1-200	0.13 μM	5	This work
Colorimetry	0.05-80	0.05 μM	10	4
Colorimetry	0-10	22 nM	30	5
Colorimetry	1000-4000	Not given	5	6
Fluorometry	0-40000	8 nM	Not given	7
Fluorometry	0.03-60	Not given	120	8
Fluorometry	0-10000	Not given	Not given	9
Fluorometry	0.2-30	62 nM	Not given	10
Fluorometry	0.06-10	20 nM	15	11
Fluorometry	0-10	0.3 μM	3	12
Fluorometry	10-100	0.83 μM	5	13
Fluorometry	0-2000	0.2 μM	6	14
Fluorometry	0.8-10	0.5 μM	Not given	15
Fluorometry	0.5-6	0.38 μM	30	16
Fluorometry	0.5-100	0.15 μM	6	17

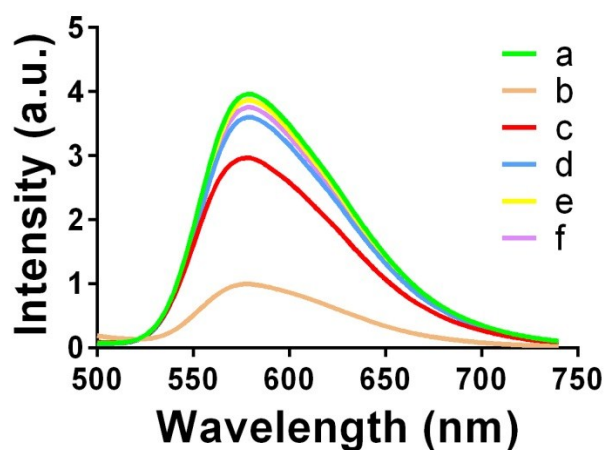


Fig. S1 Luminescence spectra of **1** in the presence of MnO₂ nanosheet or GSH. a) 10 μ M complex **1**, b) 10 μ M complex **1** + 80 μ M MnO₂ nanosheet, c) 10 μ M complex **1** + 80 μ M MnO₂ nanosheet + 200 μ M GSH, d) 10 μ M complex **1** + 80 μ M MnO₂ nanosheet + 1000 μ M GSH, e) 10 μ M complex **1** + 200 μ M GSH and f) 10 μ M complex **1** + 1000 μ M GSH.

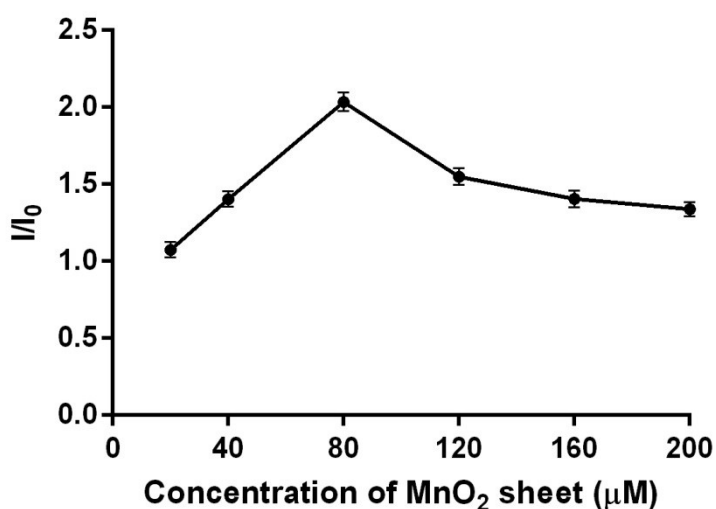


Fig. S2 The luminescence responses of **1**/MnO₂ nanosheet in the presence of or absence of GSH (100 μ M) with the different concentrations of MnO₂ nanosheet (20, 40, 80, 120, 160 and 200 μ M). I is the signal of MnO₂ nanosheet with different concentrations in presence of GSH, I_0 is the signal in absence of GSH.

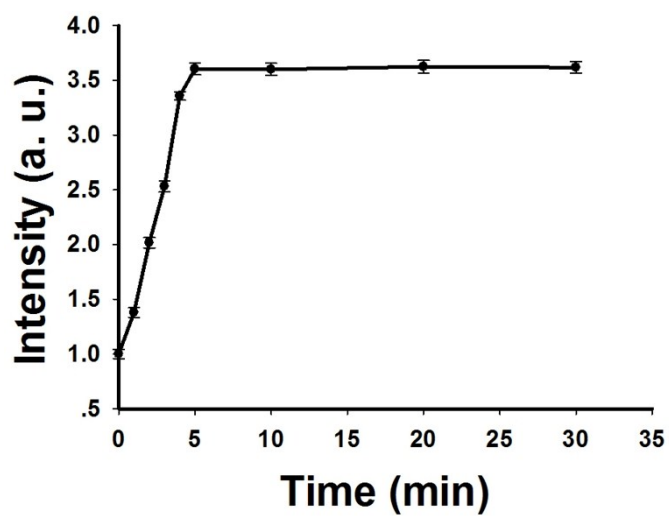


Fig. S3 The time-dependent experiment of **1**/MnO₂ nanosheet in the presence of 1 mM of GSH, with 10 μM of complex **1**.

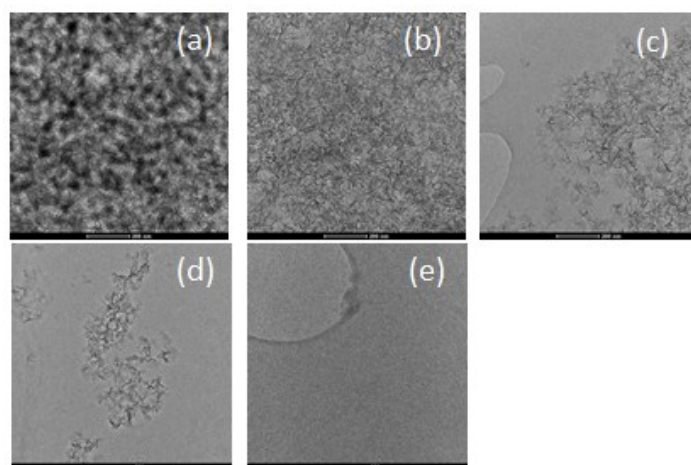


Fig. S4 TEM images of the prepared MnO₂ nanosheet (8 mM) with complex **1** in the presence of (a) 0 mM GSH, (b) 5 mM GSH, (c) 10 mM GSH, (d) 25 mM GSH and (e) 50 mM GSH.

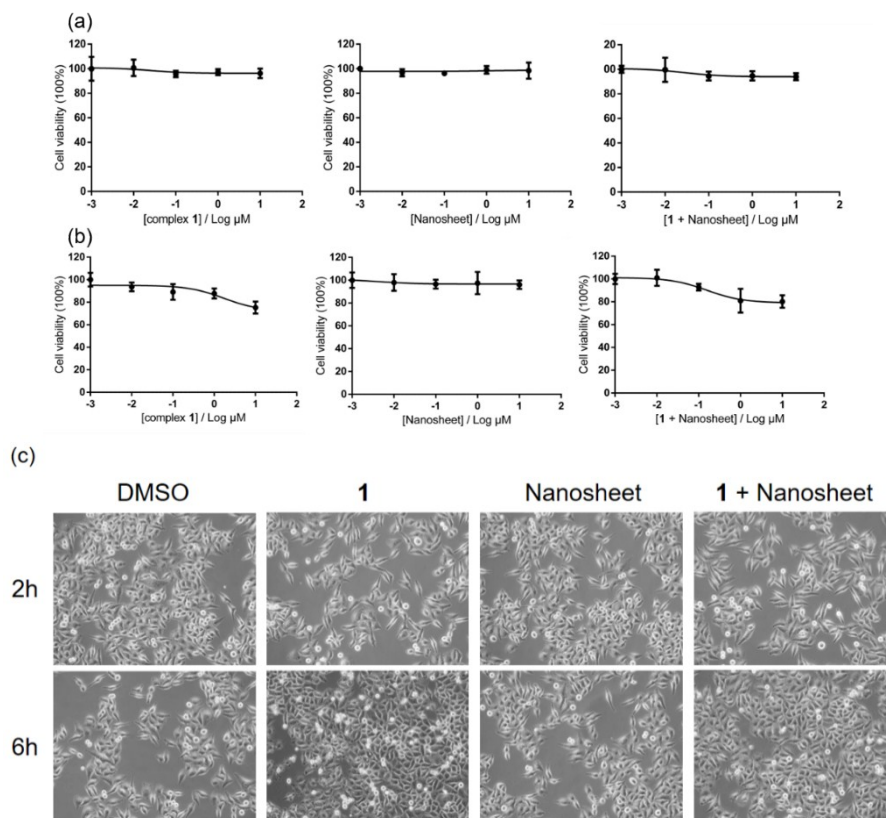


Fig. S5 The cytotoxicity effect of complex **1** (10 μM), MnO₂ nanosheet (80 μM) and complex **1** in the presence of 80 μM MnO₂ nanosheet, towards HeLa cells as determined by (a and b) an XTT assay and (c) cell imaging experiment. HeLa cells were treated with complex **1**, or MnO₂ nanosheet or complex **1** + 80 μM MnO₂ nanosheet for (a) 2 h or (b) 6 h.

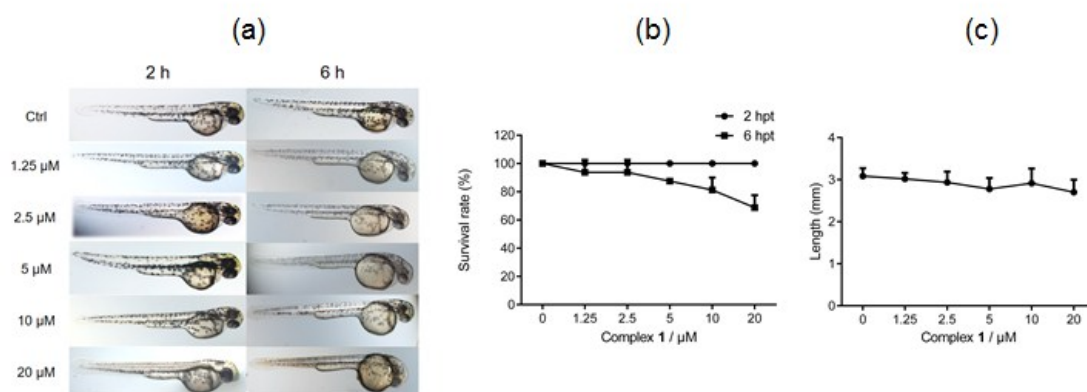


Fig. S6 (a) The representative image and (b) survival rate of zebrafish embryos after treatment with different concentrations of complex **1** in the presence of 80 μ M MnO₂ nanosheet at 2 hpt and 6 hpt (hour post treatment), (c) The body length of zebrafish embryos after treatment with different concentrations of complex **1** at 6 hpt. Embryos receiving 0.1% DMSO served as a vehicle control. Data are presented as the percentage of control in mean \pm SD.

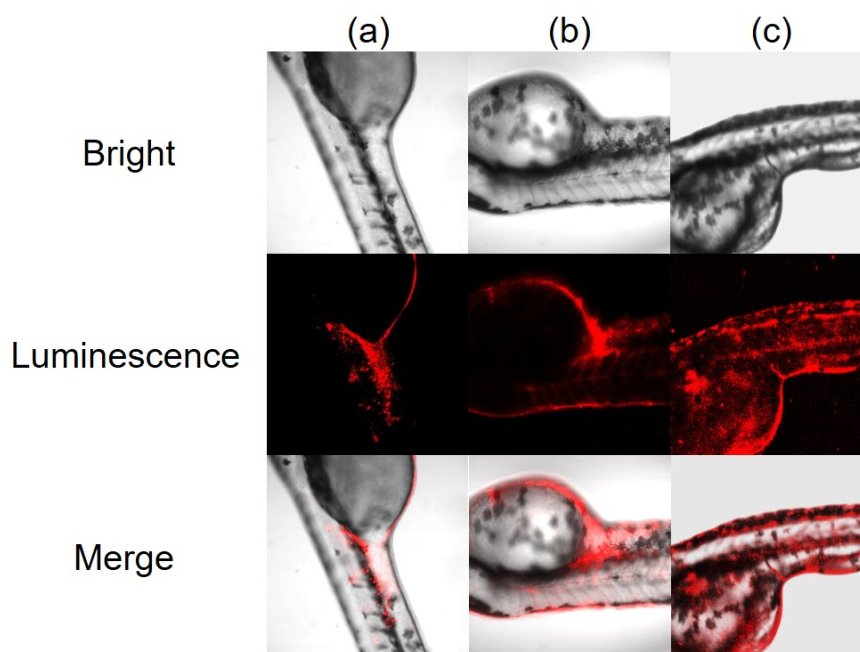


Fig. S7 Luminescence images of zebrafish incubated with complex **1** (10 μ M) for (a), (b) zebrafish blood vessel and (c) skin. Zebrafish embryos were treated with complex **1** at 72 hpf, followed by imaging at 75 hpf.

Reference

1. G. A. Crosby and J. N. Demas, *J. Phys. Chem.*, 1971, **75**, 31-31.
2. K. Kai, Y. Yoshida, H. Kageyama, G. Saito, T. Ishigaki, Y. Furukawa and J. Kawamata, *J. Am. Chem. Soc.*, 2008, **130**, 15938-15943.
3. Q. Zhao, S. Liu, M. Shi, C. Wang, M. Yu, L. Li, F. Li, T. Yi and C. Huang, *Inorg. Chem.*, 2006, **45**, 6152-6160.
4. P. Ni, Y. Sun, H. Dai, J. Hu, J. Shu, Y. Wang and L. Zhuang, *Biosens. Bioelectron.*, 2014, **63C**, 47-52.
5. M. Shamsipur, A. Safavi and Z. Mohammadpour, *Sensor. Actuat. B-Chem.*, 2014, **199**, 463-469.
6. Y. Shi, Y. Pan, H. Zhang, Z. Zhang, M. J. Li, C. Yi and M. Yang, *Biosens. Bioelectron.*, 2014, **56**, 39-45.
7. L. Zhou, Y. Lin, Z. Huang, J. Ren and X. Qu, *Chem. Commun.*, 2012, **48**, 1147-1149.
8. M. Wei, P. Yin, Y. Shen, L. Zhang, J. Deng, S. Xue, H. Li, B. Guo, Y. Zhang and S. Yao, *Chem. Commun.*, 2013, **49**, 4640-4642.
9. S. Banerjee, S. Kar, J. M. Perez and S. Santra, *J. Phys Chem. C.*, 2009, **113**, 9659-9663.
10. Q. H. Li, L. Zhang, J. M. Bai, Z. C. Liu, R. P. Liang and J. D. Qiu, *Biosens Bioelectron.*, 2015, **74**, 886-894.
11. T. H. Chen and W. L. Tseng, *Small*, 2012, **8**, 1912-1919.
12. J.-J. Liu, X.-R. Song, Y.-W. Wang, A.-X. Zheng, G.-N. Chen and H.-H. Yang, *Anal. chim. acta.*, 2012, **749**, 70-74.
13. L. Zhang and X. W. Lou, *Chemistry*, 2014, **20**, 5219-5223.
14. X. L. Zhang, C. Zheng, S. S. Guo, J. Li, H. H. Yang and G. Chen, *Anal. Chem.*, 2014, **86**, 3426-3434.
15. P. Yang, Q. Z. Xu, S. Y. Jin, Y. Zhao, Y. Lu, X. W. Xu and S. H. Yu, *Chemistry*, 2012, **18**, 1154-1160.
16. Z. Na, Q. Fei, Q. L. Hong and N. B. Li, *Biosens. Bioelectron.*, 2013, **42C**, 214-218.
17. X. Yan, Y. Song, C. Zhu, J. Song, D. Du, X. Su and Y. Lin, *Acs Appl. Mater. Interface*, 2016, **8**, 21990-21996.